

RECURRING MOLECULAR ALIGNMENT INDUCED BY PULSED NONRESONANT LASER FIELDS

Long CAI and Břetislav FRIEDRICH^{1,*}

Department of Chemistry and Chemical Biology, Harvard University, Cambridge, MA 02138, U.S.A.; e-mail: ¹ brich@chemistry.harvard.edu

Received January 29, 2001

Accepted April 10, 2001

We examine the rotational wavepackets created by the nonadiabatic interaction of a linear molecule with a pulsed nonresonant laser field. We map out the recurrences of the wavepackets and of the concomitant alignment as a function of the duration and intensity of the laser pulse. We derive an analytic solution to the time-dependent Schrödinger equation in the short-pulse limit and find it to agree quantitatively with our numerical computations. This indicates that the recurrences are favored under an impulsive transfer of action from the radiative field to the molecule. The recurring wavepackets afford field-free alignment of the molecular axis.

Keywords: Nonresonant induced dipole interaction; Polarizability anisotropy; Hybridization of rotational states; Pulsed laser fields; Alignment of molecular axis; Recurrences; Wave functions; Schrödinger equation; Quantum chemistry.

The pursuit of means to manipulate molecular trajectories and reaction pathways is a leading frontier of chemical physics. Among recent developments are methods to control the orientation and alignment of molecules¹ as well as methods to deflect and focus their translational motion² and to attain molecular trapping³. At the core of these methods is the nonresonant polarizability interaction.

The nonresonant polarizability interaction of a radiative field with a nonspherical molecule is governed by an induced dipole potential proportional to $\cos^2 \theta$, with θ the polar angle between the molecular axis and the field vector, ϵ (refs⁴⁻⁶). The $\cos^2 \theta$ potential hybridizes the rotational states, $|J, M\rangle$, of the molecule, by mixing J s that differ by 0 and ± 2 . The mixing lends the hybrid states a directionality which exhibits an end-for-end symmetry, a consequence of the double-well character of the $\cos^2 \theta$ potential. Such a directionality is termed alignment and, for a given state, is specified by the expectation value $\langle \cos^2 \theta \rangle$, the alignment cosine. The alignment cosine is a measure of the alignment of the molecular axis with respect to the

field vector ε and yields the angular amplitude of the molecular axis, $\arccos [(\cos^2 \theta)]^{1/2}$. Since the polarizability interaction is rather weak (see below), strong fields are required to attain a significant alignment. Fields of the requisite strength can be attained by focusing a pulsed nonresonant laser beam. For most small diatomic molecules, laser intensities ranging between 10^9 and 10^{13} W/cm² suffice to generate an alignment that corresponds to an angular amplitude of the molecular axis of about $\pm 30^\circ$ for the lowest molecular state⁴. However, such radiative fields are time-dependent, delivered as pulses, with nearly Gaussian time profiles. Depending on the width of the time profile (the pulse duration, τ) we distinguish two limiting cases of the interaction of the radiative field with the molecule⁷: (i) If $\tau \approx 5\hbar/B$ (where B is the rotational constant of the molecule), the interaction is adiabatic and the molecule behaves as if the radiative field were static at any instant. The states thereby created are the stationary *pendular states*⁴ (see also below). (ii) For $\tau \approx \hbar/B$, the time evolution is nonadiabatic and so the molecule ends up in a rotational wavepacket. The wavepacket comprises a finite number of free-rotor states and thus may recur after the pulse has passed – giving rise to alignment under field-free conditions, as pointed out by Bandrauk⁸ and later analyzed by others^{7,9}.

In this Communication we examine the states created by the *nonadiabatic* interaction of a linear molecule with a pulsed nonresonant laser field. We map out the molecular alignment as a function of the pulse duration and laser intensity and derive an analytic solution to the time-dependent Schrödinger equation in the short-pulse limit. This we find to agree quantitatively with our numerical computations, which indicates that the rotational wavepacket forms under an angular momentum “punch” delivered to the molecule by the radiative field. Throughout our analysis we use reduced, dimensionless variables which characterize the nonresonant polarizability interaction for any linear molecule.

THEORY

We consider a $^1\Sigma$ rotor molecule with polarizability components α_{\parallel} and α_{\perp} parallel and perpendicular to the molecular axis and a permanent dipole moment μ (if any) along the molecular axis. The molecule is subject to a pulsed plane-polarized nonresonant laser field, ε (Fig. 1). Because of the azimuthal symmetry about the field vector, the resulting induced dipole potential involves just the polar angle θ between the molecular axis and the field direction, and M , the projection of the molecular angular momentum J on the field direction, is a “good” quantum number. We limit consider-

ation to a pulsed plane-wave radiation of frequency ν and time profile $g(t)$ such that

$$\varepsilon^2(t) = \frac{8\pi}{c} I g(t) \cos^2(2\pi\nu t), \quad (1)$$

where I is the peak intensity. We assume the oscillation frequency ν to be far removed from any molecular resonance and much higher than either τ^{-1} or the rotational periods. The resulting effective Hamiltonian, $H(t)$, is thus averaged over the rapid oscillations. This cancels the interaction between μ and ε (see ref.¹⁰ for an analysis of when this occurs) and reduces the time dependence of ε to that of the time profile,

$$\langle \varepsilon^2(t) \rangle = \frac{4\pi}{c} I g(t).$$

As a result, the Hamiltonian becomes

$$H(t) = B[\mathbf{J}^2 - \Delta\omega(t) \cos^2\theta - \omega_{\perp}(t)], \quad (2)$$

where the dimensionless interaction parameters are given by

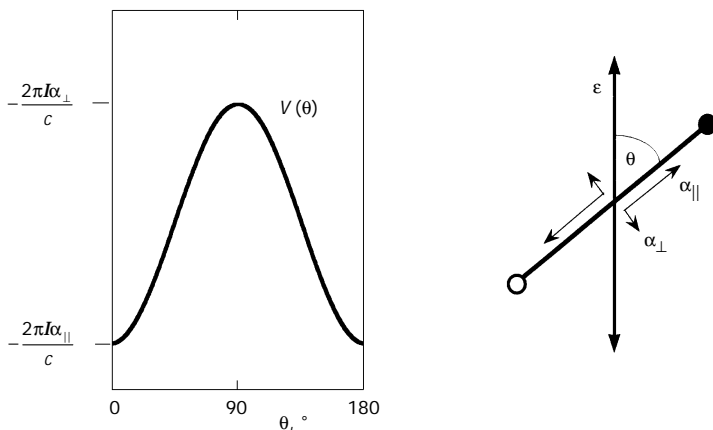


FIG. 1

The $V_{\alpha}(\theta) = (2\pi I/c)[(\alpha_{\parallel} - \alpha_{\perp}) \cos^2\theta + \alpha_{\perp}]$ induced dipole potential, with the quantities defined in the diagram on the right. The pair of potential minima in the polar regions is separated by an equatorial barrier. Note that $V_{\alpha}(0^{\circ}) = V_{\alpha}(180^{\circ}) = -2\pi I\alpha_{\parallel}/c$ and $V_{\alpha}(90^{\circ}) = -2\pi I\alpha_{\perp}/c$

$$\begin{aligned}\omega_{\parallel,\perp}(t) &= \omega_{\parallel,\perp}g(t) \\ \omega_{\parallel,\perp} &\equiv 2\pi\alpha_{\parallel,\perp}I/Bc \\ \Delta\omega &\equiv \omega_{\parallel} - \omega_{\perp} \\ \Delta\omega(t) &= \omega_{\parallel}(t) - \omega_{\perp}(t) \equiv \Delta\omega g(t) .\end{aligned}\quad (3)$$

The time-dependent Schrödinger equation corresponding to Hamiltonian (2) can be cast in a dimensionless form

$$i \frac{\hbar}{B} \frac{\partial \psi(t)}{\partial t} = \frac{H(t)}{B} \psi(t) \quad (4)$$

which indicates that \hbar/B plays the role of a reduced time. The solutions of Eq. (4) can be expanded in a series of field-free rotor wave functions $|J, M\rangle \equiv Y_{J,M}$ (pertaining to eigenenergies E_J)

$$\psi(\Delta\omega(t)) = \sum_J c_J(\Delta\omega(t)) |J, M\rangle \exp\left[-\frac{iE_J t}{\hbar}\right], \quad (5)$$

whose time-dependent coefficients, $c_J(\Delta\omega(t))$, solely determine the solutions at given initial conditions (in the interaction representation). We take the pulse shape function to be a Gaussian

$$g(t) = \exp(-t^2/\sigma^2), \quad (6)$$

characterized by a full width at half maximum, $\tau = 2(\ln 2)^{1/2} \sigma \approx 5/3\sigma$, the "pulse duration". Thus the Hamiltonian becomes

$$H(t) = B[J^2 - (\Delta\omega \cos^2 \theta + \omega_{\perp}) \exp(t^2/\sigma^2)] \quad (7)$$

and the expansion (or *hybridization*) coefficients c_J can be found from the differential equations

$$\begin{aligned}i \frac{\hbar}{B} \dot{c}_J(t) &= \\ &= -\sum_{J'} c_{J'}(t) \langle J, M | \Delta\omega \cos^2 \theta + \omega_{\perp} | J', M \rangle \exp\left[-\frac{i(E_{J'} - E_J)t}{\hbar}\right] \exp(-t^2/\sigma^2) .\end{aligned}\quad (8)$$

By taking into account the non-vanishing matrix elements $\langle J, M | \cos^2 \theta | J, M \rangle$ (see Appendix), Eq. (8) reduces to a tridiagonal form and can be numerically solved by standard methods⁷. In what follows, we consider the molecule to be in the ground rotational state, $|0, 0\rangle \equiv Y_{0,0}$, before sending in the laser pulse (i.e., for $\omega_{||,\perp}(t=0) = 0$).

We investigate the effect of both the time extent (pulse duration τ) and magnitude ($\Delta\omega$, proportional to the laser intensity I) of the laser pulse on the solutions of Eq. (8) in the short-pulse limit. First, however, we briefly review the long-pulse limit.

Long-pulse (adiabatic) limit. For $\sigma \rightarrow \infty$, the time profile $g(t) \rightarrow 1$ and Hamiltonian (7) becomes

$$\frac{H(t)}{B} = \mathbf{J}^2 - (\Delta\omega \cos^2 \theta + \omega_{\perp}). \quad (9)$$

Its stationary solutions (*pendular states*) are

$$\Psi(\Delta\omega) = \sum_J c_J(\Delta\omega) |J, M\rangle \equiv |\tilde{J}, M; \Delta\omega\rangle, \quad (10)$$

that pertain to eigenvalues

$$\lambda_{\tilde{J},M} = E_{\tilde{J},M}^z/B + \omega_{\perp}. \quad (11)$$

For $\Delta\omega = 0$, the eigenproperties become those of a field-free rotor; the eigenfunctions then coincide with spherical harmonics, and the eigenvalues become $\lambda_{J,M} \rightarrow E_{J,M}^z/B = J(J+1)$. The eigenstates can thus be labeled by M and the nominal value \tilde{J} , designating the angular momentum of the field-free rotor state that adiabatically correlates with the high-field hybrid function. In the high-field limit, $\Delta\omega \rightarrow \infty$, the range of θ is confined near a potential minimum and Eq. (9) reduces to that for a two-dimensional angular harmonic oscillator (harmonic librator). Figure 2 shows the purely attractive interaction potential, $-\Delta\omega \cos^2 \theta + \omega_{\perp}$, the energy levels $E_{\tilde{J},M}^z/B$, and the wavefunctions $|J, M; \Delta\omega\rangle$ for $\alpha_{||}/\alpha_{\perp} = 2$ and $\Delta\omega = 3$. The anisotropic part, governed by $\Delta\omega$, produces a double well which splits the pendular states bound by these wells into tunneling doublets, see e.g., the $\tilde{J}_M = 0_0$ and 1_0 pair. The amplitude of the wells and thus the number of bound states increases with $\Delta\omega$, so it grows quadratically with field strength and linearly with laser intensity. The ω_{\perp} term introduces a linear shift of the po-

and of the energy levels and has no effect on the wavefunctions. The correlations with the field-free rotor states and the harmonic liblator states $N_{|M|}$ are also indicated in Fig. 2. The uncertainty principle for the harmonic pendular oscillations can be cast in the form $\langle J^2 \rangle \langle \theta^2 \rangle > (N + 1)^2$ which implies that, for a given N , achieving a narrow angular confinement requires a wide range of J in the pendular wave function.

Short-pulse (nonadiabatic) limit. For $\sigma \rightarrow 0$, the time evolution of the initial wave-function $Y_{0,0}$ under the Hamiltonian (7) is approximated, up to order σ , by a propagator $S(t) = \exp[-i/\hbar \int H(t') dt']$, which yields an approximate wavefunction

$$\bar{\psi}(t) = \exp\left[-\frac{i}{\hbar} \int H(t') dt'\right] Y_{0,0} = \exp\left\{-\frac{i}{\hbar} B[tJ^2 - \Delta\omega \cos^2 \theta G(t)]\right\} Y_{0,0} \quad (12)$$

with $G(t) = \int_{-\infty}^t g(t') dt' = 1/2\pi^{1/2} \sigma[1 + \text{erf}(t/\sigma)]$, see also refs^{11,12}. For $t \gtrsim 12\sigma \equiv t_a$, $G(t_a)$ is of the order σ and the effect of J^2 can be neglected. As a result, we obtain

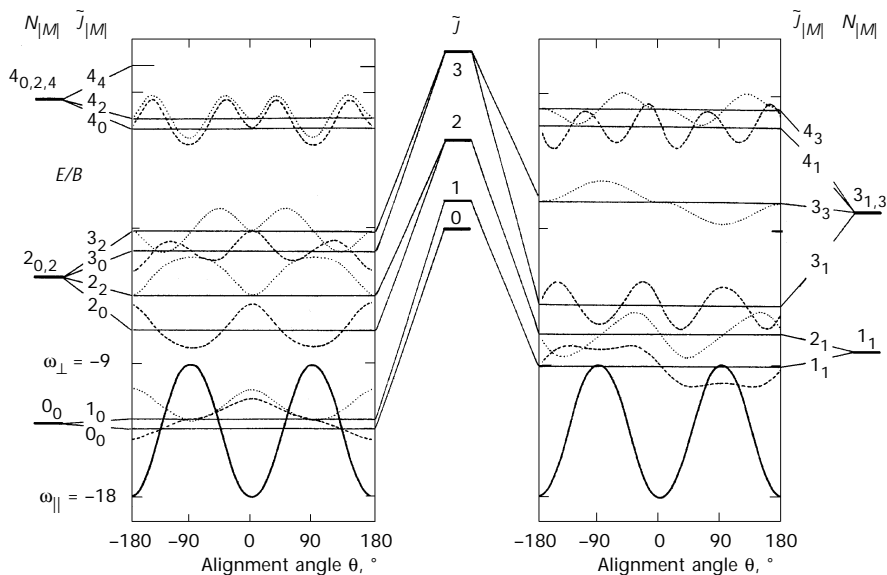


FIG. 2

Energy levels (in units of the rotational constant B) and wavefunctions (dashed and dotted curves) for the induced dipole potential $V_\alpha(\theta)$ (solid curves). For this example, with $\Delta\omega = 3$ and $\alpha_{||}/\alpha_{\perp} = 2$, only the 0_0 , 1_0 and 1_1 states are bound by the potential. Also indicated is the correlation between the states of a field-free rotor and a harmonic liblator

$$\bar{\psi}(t_a) \approx \exp \left[\frac{iB}{\hbar} \pi^{1/2} \sigma \Delta\omega \cos^2 \theta \right] Y_{0,0} . \quad (13)$$

The expansion coefficients in the non-adiabatic limit, Eq. (13), can be obtained by the transformation

$$c_J(t > t_a) \approx 2\pi \int \bar{\psi}(t_a) Y_{J,0} \sin \theta \, d\theta \equiv \bar{c}_J(t_a) . \quad (14)$$

RESULTS AND DISCUSSION

We computed the expansion coefficients $c_J(t)$ by numerically solving Eq. (8) and used them to evaluate the alignment cosine,

$$\begin{aligned} \langle \cos^2 \theta \rangle &= \sum_{J,J'} c_{J,M}(t) c_{J',M}(t) (2J+1)^{1/2} (2J'+1)^{1/2} \times \\ &\times \begin{pmatrix} J & 2 & J' \\ -M & 0 & M \end{pmatrix} \begin{pmatrix} J & 2 & J' \\ 0 & 0 & 0 \end{pmatrix} . \end{aligned} \quad (15)$$

We chose a range of $\Delta\omega$ that includes values of up to 1 000; e.g., $\Delta\omega = 240$ for KCl at 10^{12} W/cm² (ref.¹³). However, strong effects are in place at much lower $\Delta\omega$ values (see below). Note that $\sigma = 1\hbar/B$ corresponds to 5.3 ps for $B = 1$ cm⁻¹.

Figure 3 shows the dependence of the alignment cosine on time (expressed in units of σ) for different values of σ and fixed $\Delta\omega = 100$. At $\sigma = 0.01\hbar/B$ (Fig. 3a), the pulse creates a rotational wavepacket whose alignment lags behind the pulse shape function and recurs with a period determined by σ and $\Delta\omega$ (non-adiabatic behavior). At $\sigma = 1\hbar/B$ (Fig. 3c), the time dependence of $\langle \cos^2 \theta \rangle$ mimics the pulse shape function and by the time the pulse is over, the alignment of the initial wavefunction, $|0, 0; 0\rangle$, is nearly recovered. A full such recovery would correspond to the adiabatic limit when the molecule ends up in its initial eigenstate. Figure 3b shows a case when the pulse establishes a phase relationship among the components of the wavepacket that *happens* to suppress the recurrences of the alignment. Such a behavior is anomalous and reflects the accidental phase matching among the eigenstates at the end of the pulse.

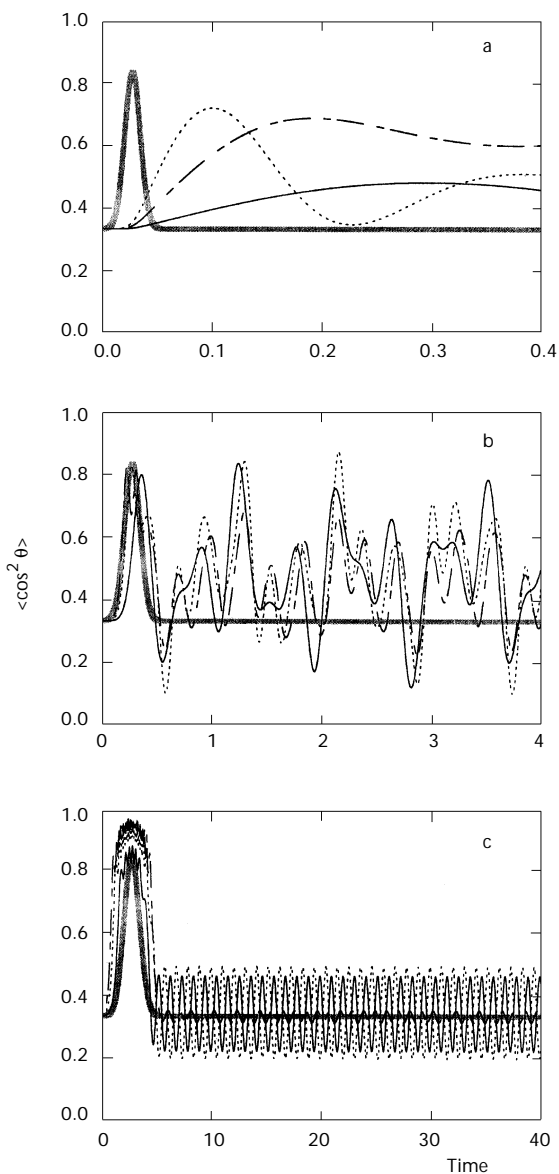


FIG. 3

Dependence of the alignment cosine on time (expressed in terms of σ) for different pulse durations $\tau \approx 5/3\sigma$ and fixed $\Delta\omega = 100$ (full line), 400 (dashed-dotted line) and 900 (dotted line). The thick curves show the pulse shape function. $\sigma = 0.01\hbar/B$ (a), $\sigma = 0.1\hbar/B$ (b) and $\sigma = 1\hbar/B$ (c)

Figure 4 shows the expansion coefficients $c_J(t_a)$ for $J \leq 6$ as a function of the induced dipole interaction parameter $\Delta\omega$ for different $\tau \approx 5/3\sigma$. The expansion coefficients pertain to a time t_a after the nonresonant laser pulse (which is centered at $t = 6\sigma$). We found that for $t \geq t_a$ the $c_J(t)$'s evolve, within $\approx 1\%$, to values which they maintain "ever after". Therefore, the $c_J(t_a)$ coefficients make it possible to fully reconstruct the wavefunction $\psi(t)$ at any time $t \geq t_a$. Figure 4a shows the $c_J(t_a)$ coefficients for $\sigma = 0.01\hbar/B$. This corresponds to a strongly non-adiabatic regime, when many of the $c_J(t_a)$ coefficients contribute to the wavefunction after the pulse passes over (up to $J = 16$ at $\Delta\omega = 900$). We also plot (thick curves) the approximate $\bar{c}_J(t_a)$ coefficients obtained in the non-adiabatic limit, Eq. (14). The agreement with the exact results is excellent, just within a few per cent. This implies that the interaction at $\sigma = 0.01\hbar/B$ is governed, over a wide range of field strengths, by an impulsive transfer of action, A , from the radiative field to the molecule: since the angular momentum is

$$L = B \int \frac{d}{d\theta} [\Delta\omega(t) \cos^2 \theta + \omega_{\perp}(t)] dt = -B\Delta\omega G(t) \sin 2\theta, \quad (16)$$

the action becomes

$$A = \int L d\theta = B\Delta\omega G(t) \cos^2 \theta. \quad (17)$$

Therefore, the operator that creates the rotational wavepacket in the nonadiabatic limit, Eq. (13), is indeed $\exp[iA/\hbar]$. Note that the $c_J(t)$ coefficients in the non-adiabatic limit scale, at any given time, according to the value of the product $\sigma\Delta\omega$.

Figure 4c shows all the contributing $c_J(t_a)$ coefficients for a pulse with $\sigma = 1\hbar/B$. One can see that at small $\Delta\omega$, the wavefunction consists mainly of a single contribution, namely the $|0, 0; 0\rangle$ initial state. This is a signature of an adiabatic behavior when the wavefunction follows the radiative field as if it were static at any field strength along the pulse profile. As $\Delta\omega$ increases, deviations from the adiabatic behavior become evident in the augmented contributions from higher $|J, 0; 0\rangle$ states. Figure 4b pertains to the intermediate case characterized by $\sigma = 0.1\hbar/B$ when the behavior falls within neither limit and the numerical calculation is the only guide.

Figure 5 shows the time average, $\langle\langle \cos^2 \theta \rangle\rangle = \sum_J |c_J(t_a)|^2 \langle J | \cos^2 \theta | J \rangle$ of the recurring alignment cosine as a function of the laser pulse duration at fixed values of the induced dipole interaction parameter $\Delta\omega = 100, 400$ and 900 .

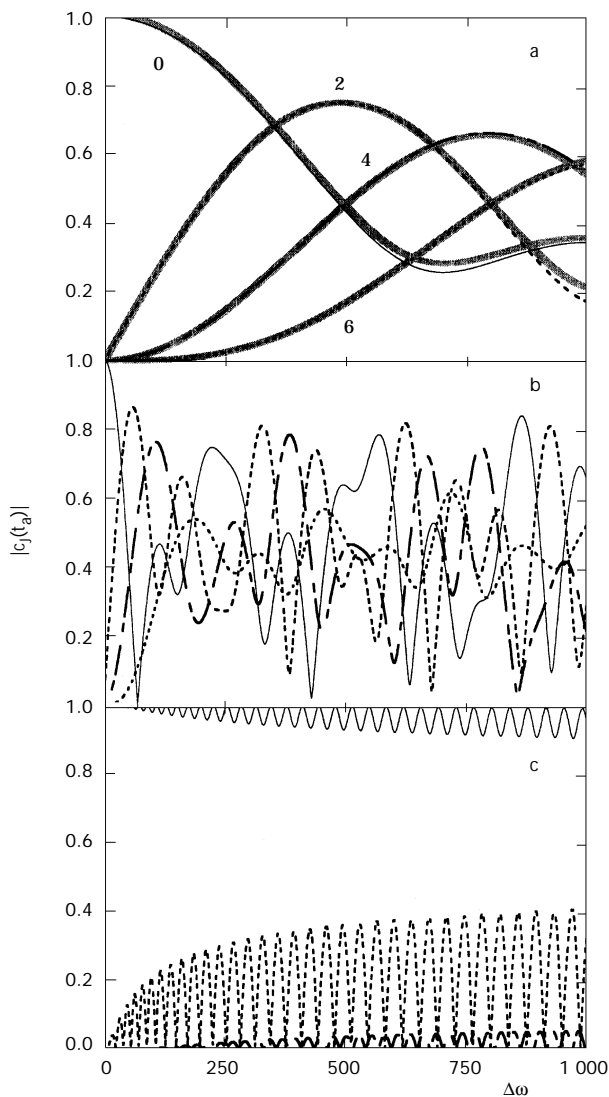


FIG. 4

Expansion coefficients $c_j(t_a)$ of the time-dependent wavefunction for $J = 0$ (full line), 2 (dashed line), 4 (dashed-dotted line) and 6 (dotted line) as a function of the induced dipole interaction parameter $\Delta\omega$ and for different pulse durations $\tau \approx 5/3\sigma$. The thick lines in a show the approximate $\bar{c}_j(t_a)$ coefficients obtained in the non-adiabatic limit, Eq. (14). $\sigma = 0.01\hbar/B$ (a), $\sigma = 0.1\hbar/B$ (b) and $\sigma = 1\hbar/B$ (c)

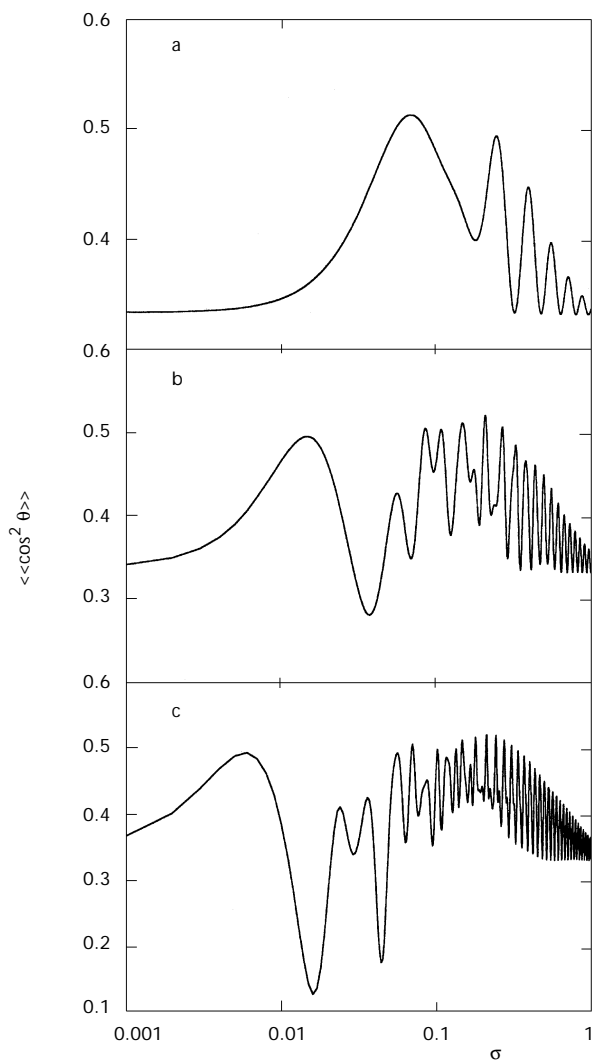


FIG. 5

Time average of the recurring alignment cosine as a function of the laser pulse duration $\tau \approx 5/3\sigma$ at fixed values of the induced dipole interaction parameter $\Delta\omega = 100$ (a), 400 (b) and 900 (c)

One can see that the alignment after the passage of the laser pulse oscillates widely, depending on σ and $\Delta\omega$. Thus, a desirable alignment cosine can be obtained by dialing the appropriate values of the σ and $\Delta\omega$ parameters. At choice values of σ and $\Delta\omega$, the alignment can reach $\langle\langle\cos^2\theta\rangle\rangle \cong 0.5$, corresponding to an angular amplitude of less than $\pm 45^\circ$. The alignment tapers off, $\langle\langle\cos^2\theta\rangle\rangle \rightarrow 1/3$, for pulses with $\sigma \rightarrow \hbar/B$ as the adiabatic limit is approached. In the adiabatic limit, the field-free molecular axis distribution is isotropic, characterized by $\langle\langle\cos^2\theta\rangle\rangle \rightarrow 1/3$.

Experimental tests of the above predictions could be carried out in an imaging double-pulse setup similar to the one of Sakai *et al.*². Using a molecule with a large rotational constant (such as, *e.g.*, CO) that can be efficiently cooled in a supersonic expansion should allow for a direct comparison of the experiment with our results, Fig. 5.

CONCLUSIONS

The strong induced dipole interaction, easily attainable with pulsed nonresonant laser fields, can be used to align nonspherical molecules. In the short pulse limit, when the pulse duration $\tau \lesssim \hbar/B$, the behavior becomes nonadiabatic and can be captured by an analytic model that renders the molecular wavefunction at any time after the laser pulse has passed. The recurrences of the wavefunctions become most prevalent if formed under an impulsive transfer of action from the radiative field to the molecule. The recurring wavepackets afford field-free alignment of the molecular axis. Whether desirable or not, the recurring molecular alignment should be taken into account in all schemes that make use of pulsed radiative fields.

APPENDIX

The non-vanishing matrix elements which enter Eq. (8) are listed below for convenience.

$$\langle J, M | J^2 | J, M \rangle = J(J+1) = \frac{E_J}{B} \quad (A1)$$

$$\langle J, M | \cos^2\theta | J, M \rangle = \frac{1}{3} + \frac{2}{3} \left(\frac{J(J+1) - 3M^2}{(2J+3)(2J-1)} \right) \quad (A2)$$

$$\begin{aligned} \langle J, M | \cos^2 \theta | J+2, M \rangle &= \frac{\sqrt{(2J+1)(2J+5)(J+1-M)}}{(2J+1)(2J+3)(2J+5)} \times \\ &\times \sqrt{(J+2-M)(J+1+M)(J+2+M)} \end{aligned} \quad (A3)$$

$$\begin{aligned} \langle J, M | \cos^2 \theta | J-2, M \rangle &= \frac{\sqrt{(2J-3)(2J+1)(J-1-M)}}{(2J-3)(2J-1)(2J+1)} \times \\ &\times \sqrt{(J-M)(J-1+M)(J+M)} \end{aligned} \quad (A4)$$

We are grateful to Dr D. Herschbach for discussions and encouragement. L. Cai thanks the Harvard College Research Fund for a grant. The support for this work has been provided by the National Science Foundation.

REFERENCES

- Herschbach D. R.: *Rev. Mod. Phys.* **1999**, 71, S411; reprinted in *More Things in Heaven and Earth: A Celebration of Physics at the Millennium* (B. Bederson, Ed.), p. 693. Springer, New York 1999.
- Sakai H., Safvan C. P., Larsen J. J., Hilligsoe K. M., Held K., Stapelfeldt H.: *J. Chem. Phys.* **1999**, 110, 10235.
- Friedrich B.: *Phys. Rev. A: At., Mol., Opt. Phys.* **2000**, 61, 025403.
- a) Friedrich B., Herschbach D.: *Phys. Rev. Lett.* **1995**, 74, 4623; b) Friedrich B., Herschbach D.: *J. Phys. Chem.* **1995**, 99, 15686.
- a) Seideman T.: *J. Chem. Phys.* **1995**, 103, 7887; b) Seideman T.: *Phys. Rev. A: At., Mol., Opt. Phys.* **1997**, 56, R17.
- Dion C. M., Keller A., Atabek O., Bandrauk A. D.: *Phys. Rev. A: At., Mol., Opt. Phys.* **1999**, 59, 1382.
- Ortigosio J., Rodriguez M., Gupta M., Friedrich B.: *J. Chem. Phys.* **1999**, 110, 3870.
- Bandrauk A. D., Claveau L.: *J. Phys. Chem.* **1989**, 93, 107; and references therein.
- Seideman T.: *Phys. Rev. Lett.* **1999**, 83, 4971.
- Keller A., Dion C. M., Atabek O.: *Phys. Rev. A: At., Mol., Opt. Phys.* **2000**, 61, 023409.
- Henriksen N. E.: *Chem. Phys. Lett.* **1999**, 312, 196.
- Cai L., Marango J., Friedrich B.: *Phys. Rev. Lett.* **2001**, 86, 775.
- Friedrich B., Herschbach D.: *J. Phys. Chem. A* **1999**, 103, 10280.



Dr B. Friedrich is Senior Research Fellow and Lecturer at Harvard University. He received his undergraduate degree from Charles University, Prague, in 1976, and his Ph.D. degree from the Heyrovský Institute of the Czechoslovak Academy of Sciences in 1981. Dr Friedrich's research interests include atomic and molecular trapping, interactions of molecules with strong static and radiative fields, cold molecular collisions, and tests of fundamental symmetries. He teaches a popular undergraduate course in experimental physical chemistry.